J Comp Physiol A (1996) 179: 29–44

ORIGINAL PAPER

D. Robert · R. N. Miles · R. R. Hoy

Directional hearing by mechanical coupling in the parasitoid fly *Ormia ochracea*

Accepted: 26 December 1995

Abstract Sound localization is a basic processing task of the auditory system. The directional detection of an incident sound impinging on the ears relies on two acoustic cues: interaural amplitude and interaural time differences. In small animals, with short interaural distances both amplitude and time cues can become very small, challenging the directional sensitivity of the auditory system. The ears of a parasitoid fly *Ormia ochracea*, are unusual in that both acoustic sensors are separated by only 520 μm and are contained within an undivided air-filled chamber. This anatomy results in minuscule differences in interaural time cues (ca. 2 μs) and no measurable difference in interaural intensity cues generated from an incident sound wave.
The tympana of both ears are anatomically coupled by a cuticular bridge. This bridge also mechanically couples the tympanana, providing a basis for directional sensitivity. Using laser vibrometry, it is shown that the mechanical response of the tympanal membranes has a pronounced directional sensitivity. Interaural time and intensity differences in the mechanical response of the ears are significantly larger than those available in the acoustic field. The tympanal membranes vibrate with amplitude differences of about 12 dB and time differences on the order of 50 μs to sounds at 90° off the longitudinal body axis. The analysis of the deflection shapes of the tympanal vibrations shows that the interaural differences in the mechanical response are due to the dynamic properties of the tympanal system and reflect its intrinsic sensitivity to the direction of a sound source. Using probe microphones and extracellular recording techniques, we show that the primary auditory afferents encode sound direction with a time delay of about 300 μs. Our data point to a novel mechanism for directional hearing in *O. ochracea* based on intertympanal mechanical coupling, a process that amplifies small acoustic cues into interaural time and amplitude differences that can be reliably processed at the neural level. An intuitive description of the mechanism is proposed using a simple mechanical model in which the ears are coupled through a flexible lever.

Key words Insect bioacoustics · Sound localization · Tympanal ear · Laser vibrometry · *Ormia ochracea*

D. Robert[1] (✉) · R. R. Hoy
Section of Neurobiology and Behavior, S.G. Mudd Hall, Cornell University, Ithaca, NY 14853-2702 USA

[1] *Present address:*
Zoologisches Institut der Universität Zürich, Winterthurerstrasse 190, CH-8057 Zürich, Switzerland

R. N. Miles
Department of Mechanical Engineering, State University of New York, Binghamton, NY 13902-6000, USA

Introduction

Time and amplitude cues for directional hearing

In animals with tympanal ears, binaural directional hearing is based on the detection of interaural time and intensity differences that are generated by a sound wave passing across the head or body (reviews: Bennet-Clark 1984; Michelsen and Larsen 1985; Middlebrooks and Green 1991). In principle, tympanal hearing organs can use time, phase, amplitude and spectral acoustic cues, singly or in combination, to detect the direction of a sound source. In the time domain, the onset time of a sound wave at one auditory organ relative to the onset at the other organ can indicate the direction of the sound source. Practically however, directional sound detection based on time and/or phase differences is limited when the distance between the ears is very short. For instance, in air an interaural distance of one centimeter produces an interaural time difference (ITD) of 30 μs. Yet, in the animal kingdom, such ITDs – and even shorter ones – are not uncommon and impose severe constraints on the peripheral and central

auditory nervous systems for reliable time coding and processing. Among several remarkable examples is the barn owl which has an intertympanal distance of about 2.5 cm (Coles and Guppy 1988) and can reliably process interaural time differences of about 10 μs (Moiseff and Konishi 1981).

Another fundamental parameter of sound that serves as a directional cue is the interaural intensity difference (IID) which arises from diffractive effects (e.g. sound shadowing) that are related to the size, density and shape of the biological tissue that surrounds and/or separates the auditory receivers. Sound shadowing also depends on the frequency of the incident sound: small objects, typically smaller than a tenth of the wavelength, have negligible diffractive effects (Morse and Ingard 1968). Hence, a body of a given size does not produce sound diffraction for relatively low frequencies but does for relatively higher frequencies.

The interaural distances of humans, birds, and insects can differ by at least a hundredfold, yet each animal can hear and localize the source of a 5 kHz tone, corresponding to a wavelength of 6.8 cm. In humans, significant IIDs of about 16 dB (at 90° azimuth) occur at 5 kHz (Schlegel 1994). In smaller animals like birds and insects, however, little or no diffractive effects are generated for lower frequencies and ITDs fall below tens of microseconds. In fact, small animals have evolved various anatomical acoustico-mechanical devices to cope with these problems for directional hearing (Hill et al. 1980; Bennet-Clark 1984; Calford and Piddington 1988; Michelsen 1994).

In some cases, sound localization does not necessarily require cues like IIDs and ITDs. In experiments of monaural directional hearing in humans, it has been shown that sound localization can be achieved by using spectral cues only (review: Middlebrooks and Green 1991). The processing of spectral information for use in directional hearing in insects has not been as well documented.

Form and function of directional sound receivers

All tympanal auditory organs that have been described so far belong to two functional categories: pressure receivers and pressure-difference receivers (Fig. 1A, B). In larger mammals, including humans, each ear is acoustically isolated (uncoupled) from the other ear and the incident sound pressure acts only on the external surface of the tympanum. Such receivers operate as *pressure receivers* (Fig. 1A). In humans, the auditory system can detect the direction of an incident sound because its relatively large interaural distance generates maximal time difference at each ear of ca. 520 μs as well as significant IIDs due to sound diffraction by the head (Middlebrooks et al. 1989; Schlegel 1994). In contrast, in small animals like birds (Hill et al. 1980; Knudsen 1980), frogs (Henson 1974; Narins et al. 1988), insects (Michel 1974) and even some mammals like moles

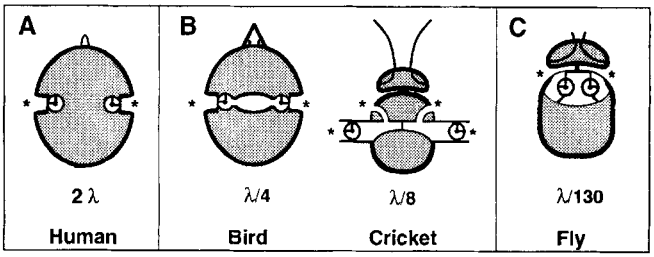

Fig. 1A–C Mechanisms of directional hearing. **A** Pressure receivers. **B** Pressure-difference receivers. **C** Mechanically coupled receivers. The ratio between the interaural distance (ID) of the animal and the wavelength (λ) at 5 kHz is given as a fraction of λ. The *asterisks* indicate the location of the sound inputs to the auditory system. In pressure receivers (**A**), variations in sound pressure are exerted only on the external side of the tympanal membrane. The two auditory organs are *acoustically isolated* by the head. In humans, the interaural distance (ID) is about twice the wavelength at 5 kHz (ca. 2 λ). In smaller animals like birds and crickets (**B**), directional hearing is based on a mechanism in which the receivers are *acoustically coupled* so that sound is transmitted from one side of the animal to the other by an internal interaural sound channel. For the *mechanically coupled* receivers (**C**), the size mismatch between the ID and λ at 5 kHz is about 130. The two auditory organs are located in the same air space, thus imposing severe limitations on the directional detection of a sound source using the conventional mechanisms of **A** and **B**

(Coles et al. 1982), the ears may be acoustically coupled by an internal air passage. The incident sound is conducted through two pathways, an *external* pathway around the head or body of the animal, and an *internal* pathway, acoustically linking the two bilateral auditory receivers. Thus, each eardrum is stimulated by external and internal sound pressures that may differ in their amplitude and phase characteristics. These acoustically coupled ears are called *pressure-difference* receivers (Fig. 1B). Such receiver systems, in effect, increase IIDs and ITDs, and hence, endow small animals with directional hearing (frogs: Eggermont 1988; Narins et al. 1988; birds: Hill et al. 1980; Knudsen 1980; crickets: Michelsen et al. 1994).

In pressure receivers, the auditory organs are located on opposite sides of the head or body and are anatomically segregated into acoustically isolated compartments, separated by dense tissue. The anatomy of pressure-difference receivers is more variable; in vertebrates, the ears are situated on both sides of the head, but in invertebrates their anatomical position varies widely (Hoy and Robert 1996). In crickets, the sound receivers are located as far apart as possible, on the tibiae of the front legs, and are internally interconnected via air filled tracheae to the thoracic spiracles (Michel 1974; e.g. Fig. 1B). The auditory system of crickets, with its complex anatomy and four identified sound inputs is the best understood pressure difference receiver system; its directional characteristics have been the focus of renewed and recent neuroethological and biophysical studies (Wendler and Löhe 1993; Löhe and Kleindienst 1994; Michelsen et al. 1994). In some

cicadas, both sensory organs and tympanal membranes are connected by an air-filled passage (Michel 1975; Young and Hill 1977) through which acoustic coupling between the two ears has been proposed (Fletcher 1992; Fonseca 1993).

The hearing organs of ormiine flies

Ormia ochracea is a parasitoid fly that acoustically locates and attacks field crickets (*Gryllus rubens* or *G. integer*; Cade 1975; Walker and Wineriter 1991). As part of their reproductive cycle, female *O. ochracea* must find cricket-hosts in which their offspring will develop. The sensory organs mediating this acoustic parasitism are tympanal ears situated on the ventral prosternum (Robert et al. 1992). In *O. ochracea*, both auditory organs are contained within a single, unpartitioned, air-filled chamber, and are separated from each other by only 520 μm (Robert et al. 1992, 1994; Edgecomb et al. 1995). For an incident pressure wave, this minute distance generates an ITD of at most 2 μs. Moreover, at 5 kHz – the natural carrier frequency of the calling song of the cricket hosts – the wavelength to interaural distance ratio is 130 (Fig. 1C); and no IIDs in the incident sound pressure could be measured with probe microphones, as predicted by theoretical and empirical studies (Morse and Ingard 1968; Michelsen 1994).

The present study shows that although interaural differences in the acoustic pressures at the tympana are extremely small, the mechanical responses of the tympana show significant differences. The mechanical response of the tympana and associated cuticular structures are examined in detail using laser vibrometry. The data presented here strongly suggest that the motions of the tympana are coupled through a cuticular structure (the intertympanal bridge) that functions like a flexible lever. We have previously proposed an analytical model of this system which indicates that a mechanical coupling between the tympana, as suggested by our data, can endow the ears with a highly directional response (Miles et al. 1995). The use of mechanical coupling between the ears of *O. ochracea* constitutes a novel mechanism for directional hearing and represents a third kind of directional receiver for terrestrial animals (Fig. 1C). The mechanical structure of the hearing organs increases the minimal acoustic interaural time and amplitude difference cues into more substancial mechanical time and amplitude difference cues that can be processed by the nervous system.

Materials and methods

Animals

The specimens used for the present study were reared from flies collected in the field near Gainesville, FL, or at the Gulf Coast Research and Education Center at Bradenton, FL. The methods of collection, culture and rearing of ormiine flies were those of Walker (1986) and Wineriter and Walker (1990).

Experimental setup

A. Positioning of the preparation

Flies were waxed (Surgident dental wax, Colombus Dental Co.) to an adjustable stage that allowed accurate positioning of the specimen relative to the sound field and a laser vibrometer. The preparation of the fly specimen for laser vibrometry required cold anesthesia and decapitation. The stage, loudspeaker, reference microphone, positioning microscope, laser optical head and its positioning stage (Fig. 2A) were bolted on a Newport Research Series (Model RS6000) vibration isolation table (dimensions: 1.32 m × 2.64 m × 0.33 m). The fly was placed at the intersection of the rotation axes X, Y and Z of the adjustable positioning stage (Fig. 2B) to make the fine spatial adjustments necessary to optimize the strength of the reflected laser optical signals. The positioning system was designed so that the loudspeaker and the specimen moved together in the azimuthal plane relative to the laser beam.

B. Laser Doppler vibrometer

The mechanical responses of the fly's hearing organs were measured with a Polytec laser vibrometer, a Polytec OFV 2100 electronics unit and Polytec OFV 300 optical sensor head. The vibrometer permits the detection of vibration velocities as low as 0.5 μm/s over a frequency range from 0.1 Hz to 500 kHz. The optical sensor head was mounted on a two-dimensional motorized micrometer stage (Oriel model 16647-16327, motor control unit 18000). The laser beam transmitted upon the fly tympana could be moved, in azimuth and

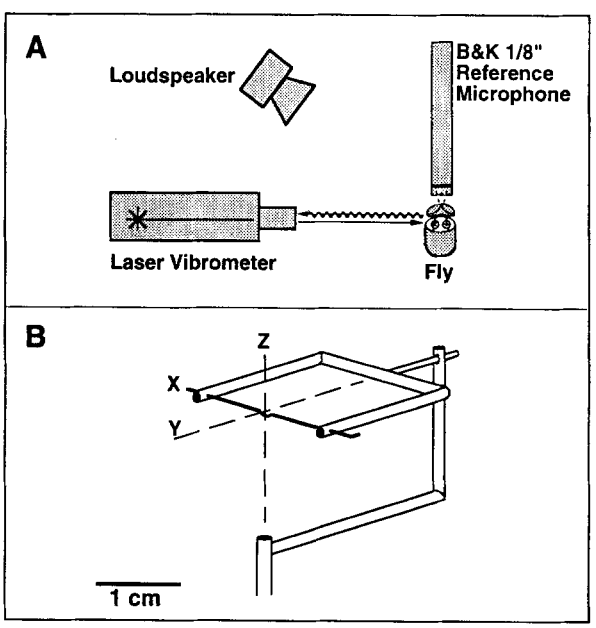

Fig. 2A, B Experimental setup for the measurement of tympanal vibrations. **A** Principal components: the laser vibrometer, the loudspeaker, the reference microphone and the fly specimen (not drawn to scale). **B** Positioning stage used to orient the fly with respect to the sound field and the laser vibrometer. The *dotted lines* indicate the axes of rotation for three-dimensional positioning

elevation with a minimal displacement of less than one micrometer. A Nikkor macrolens (55 mm, 1:2.8) was used to focus the laser beam down to a 5 μm diameter spot. Positioning of the beam was visually monitored with a Wild-Leitz M3Z stereomicroscope equipped with a Wild DM-RB633 laser filter. During measurements, the microscope was removed from the sound field.

The optical sensitivity of the vibrometer was sufficient to obtain reproducible, highly coherent data, obviating the need for glass beads or other reflective particles which would enhance the reflectivity of membranous or other cuticular structures. Thus, the measurements were done under non-loading conditions.

C. Sound stimulation

The sound stimulus was usually a 10 ms burst of band-limited random noise (bandwidth: 1–25 kHz) and overall sound pressure level of 104 dB re. 20 μPa. The stimulus was digitally synthesized by a custom-written PC-based program, band-pass filtered from 1 to 25 kHz, amplified (Brüel and Kjær (B&K) type 2706 power amplifier) and broadcast from a tweeter (ESS-AMT1). This tweeter could deliver signals over the frequency range 1–30 kHz with minimal distortions. In other measurements, sound bursts simulating the cricket calling song (*Gryllus rubens*) were used to investigate the temporal response of the hearing organs. These stimuli were 10 ms long pulses of 5 kHz carrier frequency, with onset and offset linear ramps of 1 ms. All stimuli could be delivered to the specimen at angles of incidence ranging from $-90°$ to $+90°$ azimuth.

D. Acoustic calibration

The sound pressure at the ears was monitored with a B&K type 4138 condenser microphone (operated with a B&K type 5935 power supply and amplifier). This reference microphone, placed directly above (< 2 mm) the fly specimen, measured as precisely as possible the sound pressure applied to the ears (Fig. 2A). The small 1/8″ microphone did not interfere with the sound field in the frequency range applied here. The signal from the reference microphone was used to measure any distortions introduced by the tweeter, and the pressure of the incident sound used to compute the transfer functions and coherence functions (see signal processing methods). The sound pressure at the location of the fly was used to assess the build-up of standing waves due to reflective and/or diffractive experimental conditions and to indicate the level of confidence with which the acoustic conditions can be considered "free-field". Within an 1.5×1.5 cm area around the preparation, the sound field was found to be homogenous within 2 dB over the frequency range investigated.

Similar measurements were carried out in the electrophysiological setup to investigate the diffractive alterations of the sound field in the close proximity of the fly's body. In one set of experiments, a B&K type 4138 condenser microphone was mounted on a micromanipulator and scanned over a 2×2 cm area around the fly, and in the absence of the fly, for two different frequencies (Fig. 3). These measurements established that maximal sound pressure heterogeneities at the location of the fly did not exceed 1 dB. These measurements also show that the fly causes negligible diffraction in the sound field at 5 and 20 kHz. In another experiment, two probe microphones were used to assess the sound pressure and the time of arrival of sound waves at the hearing organs. These probe microphones were customized Knowles miniature microphones (type 3068) fitted with steel tubing, the tip of which was 100 μm in diameter. The frequency response of these probe microphones restricted their use to frequencies below 10 kHz. The phase responses for the two probe microphones were cross-calibrated by positioning their tips at the same point in the sound field to obtain a phase correction factor.

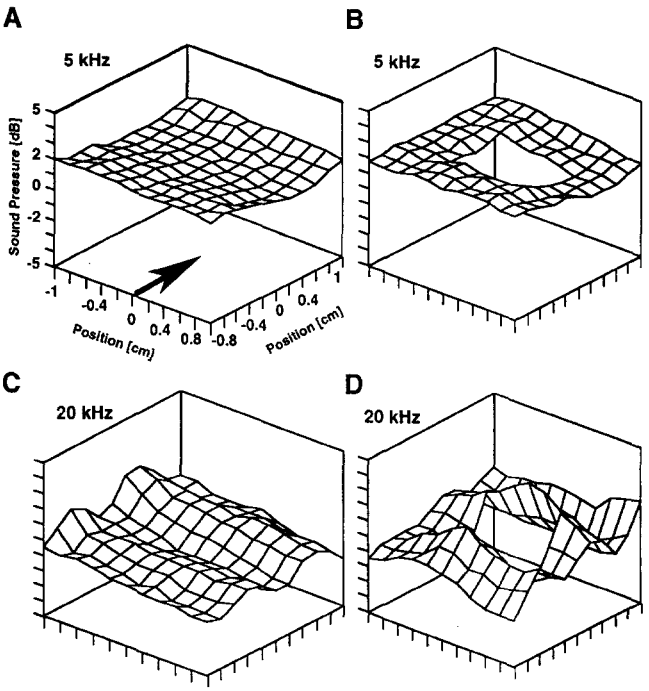

Fig. 3A–D Assessment of the quality of the sound field. The sound pressure was measured for 5 kHz (**A**, **B**) and 20 kHz (**C**, **D**). **A**, **C** Without the fly. **B**, **D** With the fly in the sound field. The position (0; 0) in the measuring grid is the center of the fly's prothorax. For **B** and **D** the hole in the grid is where the fly is located. The *arrow* in **A** indicates the direction of the incident sound

E. Signal processing

Signals from the laser vibrometer and reference microphone were digitized using a Microstar 2400/6 A/D board (12 bit, 64 kHz/channel). A transient window was applied to the data in the time domain prior to analysis. Spectral analysis was performed using a Fast Fourier Transform (FFT) to calculate the cross-power spectra, auto-power spectra, and transfer functions of the membrane velocity (or displacement) values relative to the incident acoustic pressure. The spectral analysis had a frequency resolution of 31.25 Hz which was found to be sufficient given the absence of sharp resonances in the mechanical response of the tympana. The averaged responses of 10 to 15 stimulus presentations were used to compute the transfer functions between the mechanical response of the hearing organ (laser signal) and the incident sound pressure (reference microphone signal). Transfer functions were computed as the cross-power spectra between the laser and microphone signals divided by the auto-power spectra of the microphone signal. The frequency dependence of the apparent time delay was computed from the complex transfer functions.

In order to estimate the level of unrelated noise introduced in the data, a coherence function for each stimulus presentation was computed as:

$$\frac{|G_{xy}(f)|^2}{G_{xx}(f)G_{yy}(f)}$$

where $G_{xy}(f)$ is the cross-power spectrum between the laser signal $x(t)$ and the reference microphone signal $y(t)$, and $G_{xx}(f)$ and $G_{yy}(f)$ are the auto-power spectra of the laser and microphone signals respectively. The range of the coherence function is from 0 to 1, where 0 indicates the total contamination of the signal by

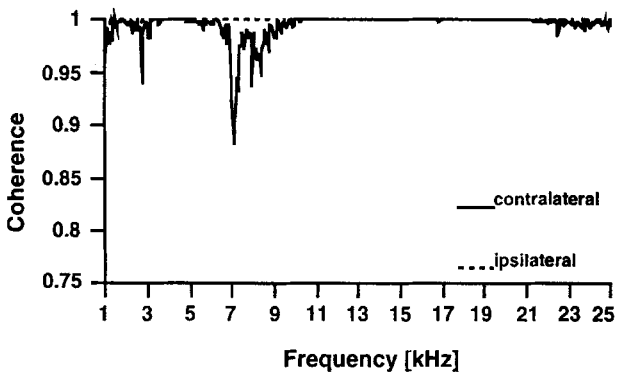

Fig. 4 Coherence as a function of frequency measured during the acoustic stimulation. Coherence value of 1 indicates that the data are not contaminated by external, unwanted noise. Ipsi- and contralateral curves are from measurements on the tympanal pits (10 averages from one animal). Data were rejected when coherence dropped below 0.8

unrelated noise, and 1 indicates the absence of unrelated noise. Coherence values were typically above 0.95 over the frequency range 1–25 kHz (Fig. 4), indicating that unrelated noise influenced the measurements by less than 5%. Similarly, the coherence between the electric signal fed to the loudspeaker and the signal from the reference microphone was always greater than 0.99.

F. Neurophysiology

The extracellular neurophysiological recordings were made using tungsten electrodes (A-M systems, 5 MΩ) implanted at the base of the frontal nerve. The frontal nerve contains the primary auditory afferents in *O. ochracea* (Robert et al. 1994). Summed evoked potentials from multiple auditory units were amplified by an A-M system model 1800 AC amplifier. In these experiments, incident sound stimuli consisted of 10 ms pulses of 5 kHz carrier frequency at 90 dB SPL (re. 20 μPa), 1 ms rise/fall time. The bilateral time delay was determined by measuring the time delay of the action potentials with reference to the signal from the reference probe microphone. The probe was placed directly in front of the tympanum and recorded the time at which the sound arrived with a precision of ±0.49 μs (sd, $n = 10$ repetitions). Sounds were delivered at 90 degrees incidence from (right or left) the longitudinal body axis while recording from one of the tympanal nerves.

Results

The anatomy of the ormiine ears

The external auditory anatomy of *O. ochracea* is shown in 5A, B and 6A. Externally, the two tympanal hearing organs are located on the fly's ventral prosternum, just behind the posterior edge of the head (Fig. 5A, black arrow), and between the neck insertion in the prothorax (N) and the prothoracic coxae (Co) (Fig. 5B). The eardrums are not simple homogeneous cuticular sheets, but are two thin (< 1 μm), corrugated prosternal tympanal membranes (PTM, black arrow) (Fig. 5B). Each tympanum is thrown with radial corrugations that converge near its midline on to a symmetrical pair of thickened cuticular flanges (Fig. 6A). These two flanges connect across the midline to form the *intertympanal bridge*. Each arm of the intertympanal bridge bears a marked distal depression, the tympanal pit (TP, Fig. 6A), to which is internally attached a chordotonal auditory sensory organ (Robert et al. 1992, 1994). Thus, there is a direct mechanical connection of the external structure converting sound energy into mechanical energy (the tympanum) to the internal mechanosensory organ (the bulba acustica).

The mechanical interaural amplitude difference

In response to sound stimulation at 45° of azimuthal angle, the amplitude of vibration of the ipsilateral tympanal membrane (the membrane nearest to the sound source) is markedly higher than that of the contralateral membrane (Fig. 6A, B). Differences in the displacement amplitude are detectable above 4–4.5 kHz and reach 10–17 dB for frequencies up to 25 kHz. In the frequency range from 4.5 to 25 kHz, the average amplitude difference between the mechanical response of ipsilateral and contralateral PTMs is 13.6 dB (sd: 4.0, $n = 881$ frequency points). As a control measure, the laser was focused on the probasisternum, a region that is made of thicker cuticle and that is not part of the

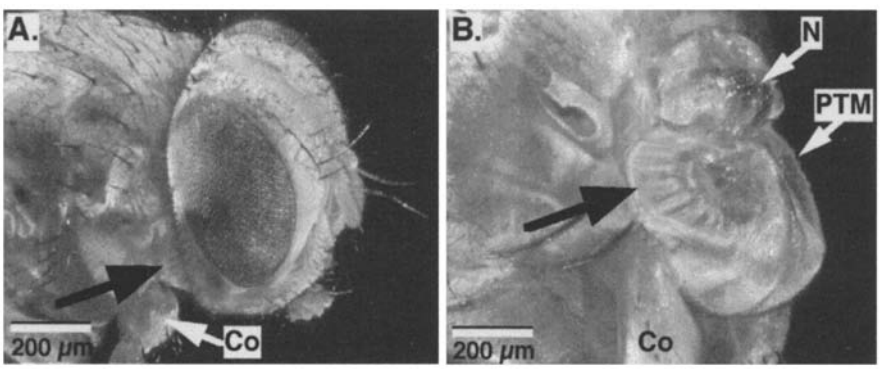

Fig. 5A, B Light scanning micrographs illustrating the external auditory anatomy of *O. ochracea*. **A** Semi-lateral view of the head and prosternum. **B** Semi-lateral view of the prosternal region with the head removed. *Co* prothoracic coxa; *N* neck; *PTM* prosternal tympanal membrane. The *black arrow* points to the lateral border of the fly's right tympanal membrane. Note the corrugations of the tympanum

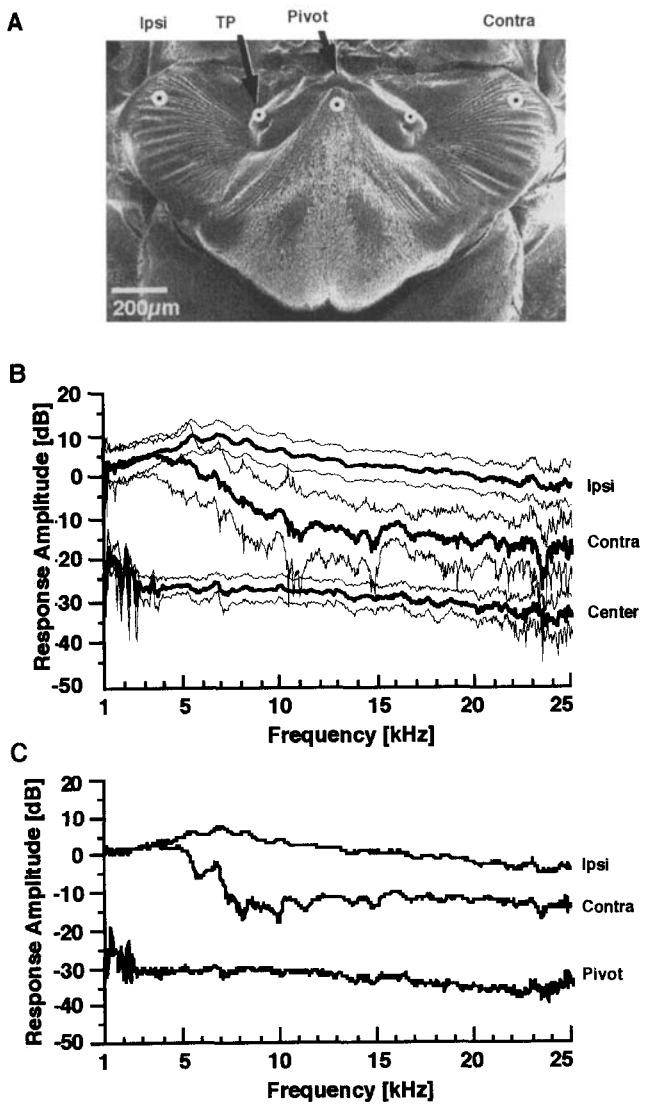

Fig. 6A–C The tympanal vibrations in response to a noise stimulus at 45° azimuth. **A** Scanning electron micrograph (frontal view) of the tympanal membranes and the intertympanal bridge of a decapitated fly. The *dots* indicate the location of the laser beam pointed at the tympanal membranes, tympanal pits (*TP*), and at the thick, cuticular probasisternum (*central dot*). **B** Amplitude displacement spectra showing the mechanical displacement of the tympanal membranes at the locations indicated in **A**. *Ipsi*: response of the ipsilateral tympanum. *Contra*: response of the contralateral tympanum. *Center*: response of the probasisternum. Amplitude of the transfer functions are given in dB re. 31.6 nm/Pa. The *thin lines* indicate ±1 standard deviation of the amplitude spectra. Ipsi- and contralateral curves: $n = 8$ animals; cuticular measurement: $n = 4$ animals. **C** Amplitude displacement spectra of the tympanal pits and the pivot point of the intertympanal bridge. Conditions same as in **B**. Ipsi, contra: $n = 5$ animals, pivot: $n = 3$ animals

tympanum (central dot, Fig. 6A). As expected, the probasisternum vibrates much less than the tympanal membranes (− 15 to − 30 dB, Fig. 6B), indicating that the measured mechanical response is not due to general vibrations of the preparation in the sound field, but solely to the displacement of the tympanal membranes. Hence, a sound stimulus delivered at 45 angle of azimuth causes both tympanal membranes to vibrate, with the ipsilateral membrane responding more strongly than the contralateral membrane at frequencies above 4 kHz.

The interaural intensity difference of the incident sound pressure measured at the location of the tympanal membranes is on the order of the measured irregularities of the sound field (< 2 dB). Therefore, it is concluded that the observed interaural difference in the mechanical response (13.6 dB) is not a result of interaural sound pressure differences acting on the PTMs (< 2 dB).

Amplitude spectra from the tympanal pits (TPs) also reveal important bilateral differences in their mechanical responses (Fig. 6C). From 4.5 to 25 kHz, the average difference in amplitude between the ipsi- and contralateral TPs is 12.4 dB (sd: 3.4, $n = 881$). These substantial differences in amplitude reflect those observed for the tympanal membranes (Fig. 6B). The point measured at the center of the intertympanal bridge (pivot, Fig. 6A) moves with a lower displacement amplitude (− 23.3 dB; sd: 4.8, $n = 881$) than that of the TPs (Fig. 6C). The mechanical responses of both PTMs and TPs conspicuously lack sharp resonant peaks, and show maximal displacement amplitudes at frequencies between 5–7 kHz (Fig. 6B, C).

The mechanical interaural time difference

The mechanical displacements of the two TPs were measured while stimulating with the simulated cricket calling song (Fig. 7A). The oscillograms of the mechanical response show that both TPs oscillate sinusoidally, closely following (cycle-by-cycle) the acoustic pressure variation of the 5 kHz stimulus (Fig. 7B).

Because the interaural distance in the fly is only 520 µm, the arrival times of the incident pressures at the TPs are delayed by less than 2 µs and have the same amplitude (Fig. 7A). However, the mechanical response of the ipsilateral TP leads that of the contralateral response by 58 µs (Fig. 7B). At 5 kHz, this represents about a quarter of the 200 µs period, or a 100.8° phase shift. For 8 animals the mean mechanical interaural delay was 48.3 ± 11.2 µs (±sd; range 35.3 to 68 µs). Under these conditions, the two TPs also oscillate with different amplitudes (Fig. 7B), independently corroborating the measurements made with random noise (Fig. 6C).

In order to understand the time dependency of the mechanical responses at different locations on the ears, transfer functions of the relative time delays were generated by subtracting the ipsilateral and contralateral phase spectra and converting the resulting phase angles into time values, as shown in Fig. 8. At 5 kHz, the time delay between the two mechanical displacements is

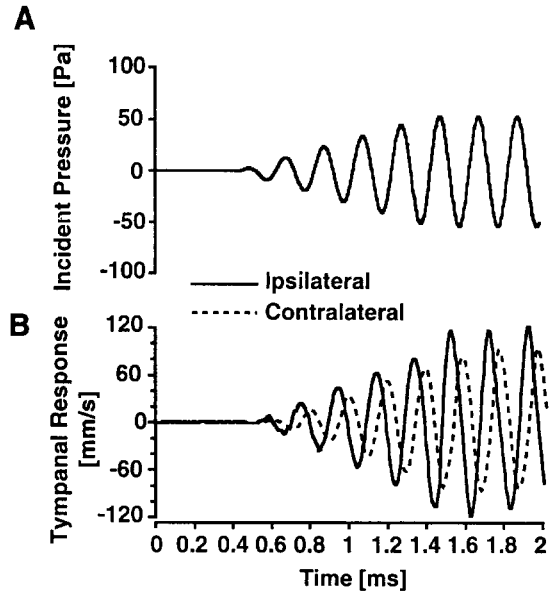

Fig. 7A, B Mechanical response measured at the tympanal pits as a function of time. The stimulus is a 5 kHz pulse (10 ms duration, 1 ms rise/fall time) delivered at 45° angle of incidence. **A** Incident sound pressure at the tympanal pits. In this situation, the delay in the time of arrival at the two tympanal pits is 1.7 μs, and is not resolved at the time scale shown. **B** Mechanical response of the tympanal pits. *Solid line*: response of the ipsilateral tympanal pit. *Dotted line*: response of the contralateral tympanal pit. Note how the mechanical response of the ipsilateral TP leads that of the contralateral TP

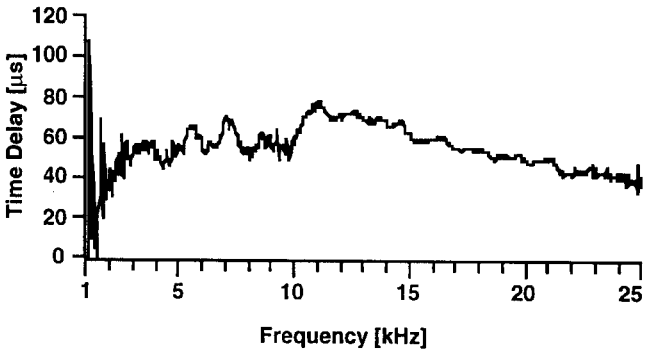

Fig. 8 Time delay between the ipsilateral and contralateral tympanal pits as a function of frequency. The angle of incidence of the random noise stimulus is 45°. The time delay is computed from the phase transfer functions ($n = 5$ animals)

57.5 μs (corresponding to a phase difference of 103.5°). In comparison, the time delay of the 5 kHz acoustic pressure at the TPs measured with the probe microphones is only 1.45 μs (sd = 0.49, $n = 10$) (corresponding to a 2.6° phase difference). These measurements independently confirm the 48.3 ± 11.2 μs delay observed with the 5 kHz simulated cricket calling song stimulus (Fig. 7B).

The response to different angles of incidence

The directional response of the fly ears was measured for different angles of the incident sound. The transfer functions of Fig. 9 show the response of the ipsilateral and contralateral TPs for angles of incidence ranging from −90° to +90° of azimuth. The interaural difference in the response amplitude decreases as the angle of incidence decreases for all frequencies tested. For a frontal sound stimulus (0°) the ipsi- and contralateral pits move with similar amplitudes, with an average difference of 2.8 dB (sd: 1.0). This small difference is probably due to the slight, unavoidable misalignment of the specimen with respect to the 0° frontal direction of the speaker. At negative angles, the curves invert, indicating that the formerly ipsilateral side becomes the side farthest from the sound source and thus vibrates at lower amplitudes. It appears that the overall amplitude response of the ipsilateral side does not vary, when compared to the changes that the contralateral side experiences (compare curves 50° to 30°, and −50° to −30°).

The time delay between the two TPs, as calculated from the complex transfer functions, reveals more of the dynamics of the mechanical response (Fig. 10). For all frequencies, the time delay decreases as the angle of incidence approaches the frontal position (0°). At 90°, the average delay between the two pits, across all frequencies, is 48.4 μs (sd: 11.6); at 5 kHz it is 55.8 μs. At 0° incidence, however, the average delay is 5.08 μs (sd: 4.2).

Plotting the difference in the mechanical response between the ipsi- and contralateral TPs as a function of the angle of incidence reveals the sensitivity of this mechanical system to the direction of an incident sound. For example, at 5 kHz, as the angle of incidence of the sound stimulus varies from +90° (or −90°) to the frontal position (0°), the difference in amplitude becomes smaller (Fig. 11A). Similarly, the time delay between the two sides of the fly's ears is directly proportional to the angle of incidence of the stimulus (Fig. 11B).

Deflection shapes

Laser measurements were systematically taken across the breadth of both ears in order to further document the dynamics of vibration of the tympanal membranes and the intertympanal bridge. The (real and complex) transfer functions between the mechanical response and the input acoustic pressure were measured for 15 locations on the PTMs and TPs in response to a random noise stimulus (Fig. 12A). The vibrations of the intertympanal bridge were measured at five different locations: one measure at each TP (points 1 and 2, Fig. 12A), one at the pivot of the intertympanal bridge

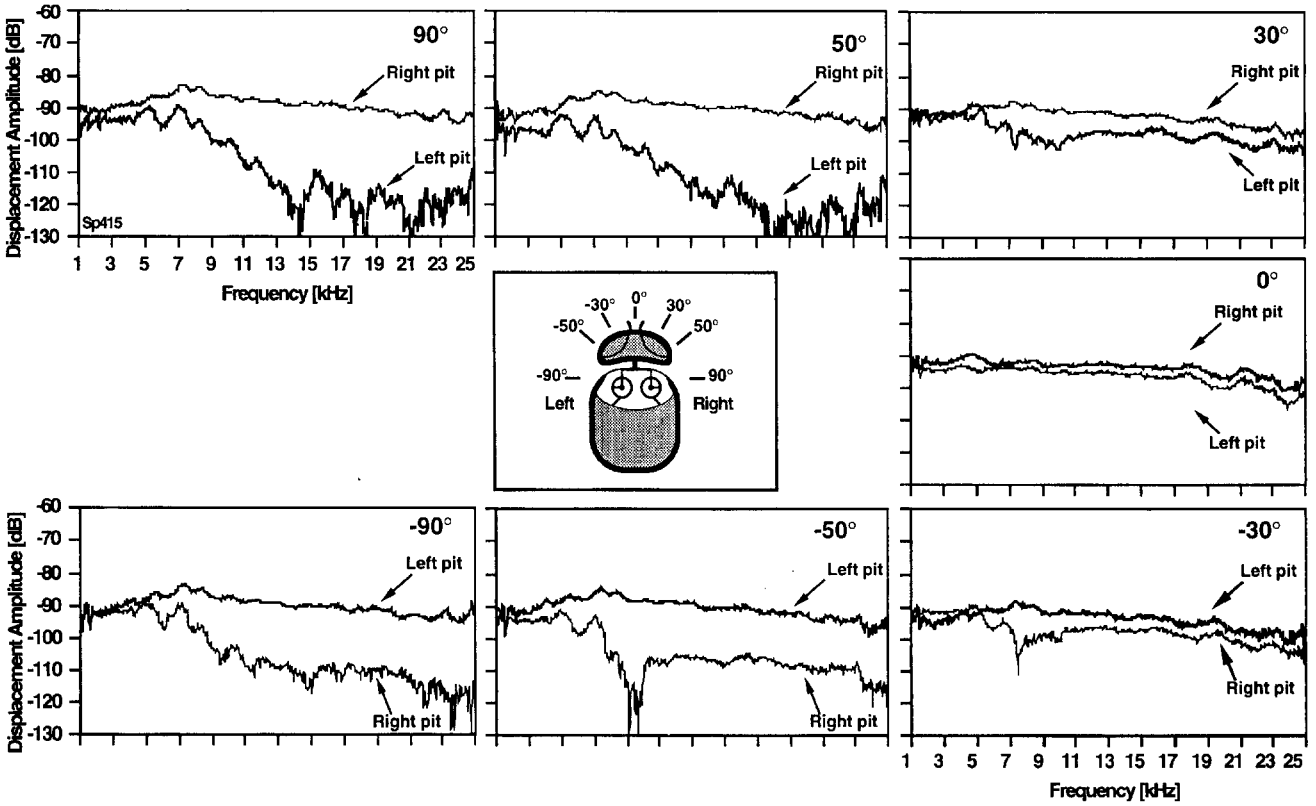

Fig. 9 Amplitude-frequency spectra at different angles of incidence of the sound stimulus. The *inset* shows the convention for orientation: 90 is to the right of the animal, 0° frontal, − 90° to the left of the animal. The mechanical responses of each tympanal pit is labeled for each angle of incidence. At 90°, the side right side is closer to the sound source and responds with a larger amplitude. The situation is reversed for negative angles of incidence. Each curve is an average of ten spectra measured on one animal. The frequency and amplitude scales are the same for all panels

(point 3, Fig. 12A), and one measure at each intermediate location between the pivot and the TPs. The deflection shapes were reconstructed by plotting the instantaneous displacement of the 15 measured locations, at three different times, along the period of a given sound frequency. In figure 12B, the deflection shapes at 5 kHz are shown for three successive times, T_1, T_2 and T_3, at the maximum outward, zero and maximum inward deflections of the ipsilateral tympanal membranes and intertympanal bridge. Times T_1, T_2 , and T_3 also correspond to three 50 μs time intervals equally spaced along the 5 kHz period (200 μs). It is clear that when the ipsilateral tympanal membranes and the ipsilateral branch of the intertympanal bridge are deflected outward (upward deflection, Fig. 12B, T_1), the contralateral side is deflected inward (right side of the deflection shape diagram). At time T_2 both sides show a small outward deflection. At time T_3, the situation is opposite to T_1. This dynamic response shows that the tympana and intertympanal bridge rock back and forth about a central, immobile pivot (point 3). Such coupled movement of both sides of the intertympanal bridge can also be visualized and demonstrated by manually deflecting one tympanal pit with a fine needle. When one tympanal pit is gently pushed inward, the other tympanal pit experiences an outward deflection.

In Fig. 13, the dynamic response of the tympana and the intertympanal bridge is shown for four different frequencies. At lower frequencies (2 kHz), the amplitude differences between the ipsi- and contralateral sides are minimal (also see Fig. 6B, C), and the ipsilateral and contralateral deflections (light peaks and dark valleys) occur relatively synchronously (Fig. 13A). At 5 kHz, the outward displacement of the ipsilateral side (light gray peak) is accompanied by an inward displacement of the contralateral side (dark gray valley) (Fig. 13B), and both displacements are of similar amplitudes (see also the response amplitude at 5 kHz in Fig. 6B, C). However, from the contour plots on the graphic's floor, it is apparent that the maximal outward displacements (lighter areas) are delayed from each other by about 57 μs at 5 kHz. The deflection shapes at 6 kHz are similar to those at 5 kHz, indicating that the tympana and intertympanal bridge are rocking about the central pivot, with a time delay of 58.5 μs (Fig. 13C). As previously seen in Fig. 6, the amplitude difference between ipsilateral and contralateral mechanical displacements is more pronounced for frequencies above 5 kHz. At higher frequencies (15 kHz), the ipsilateral

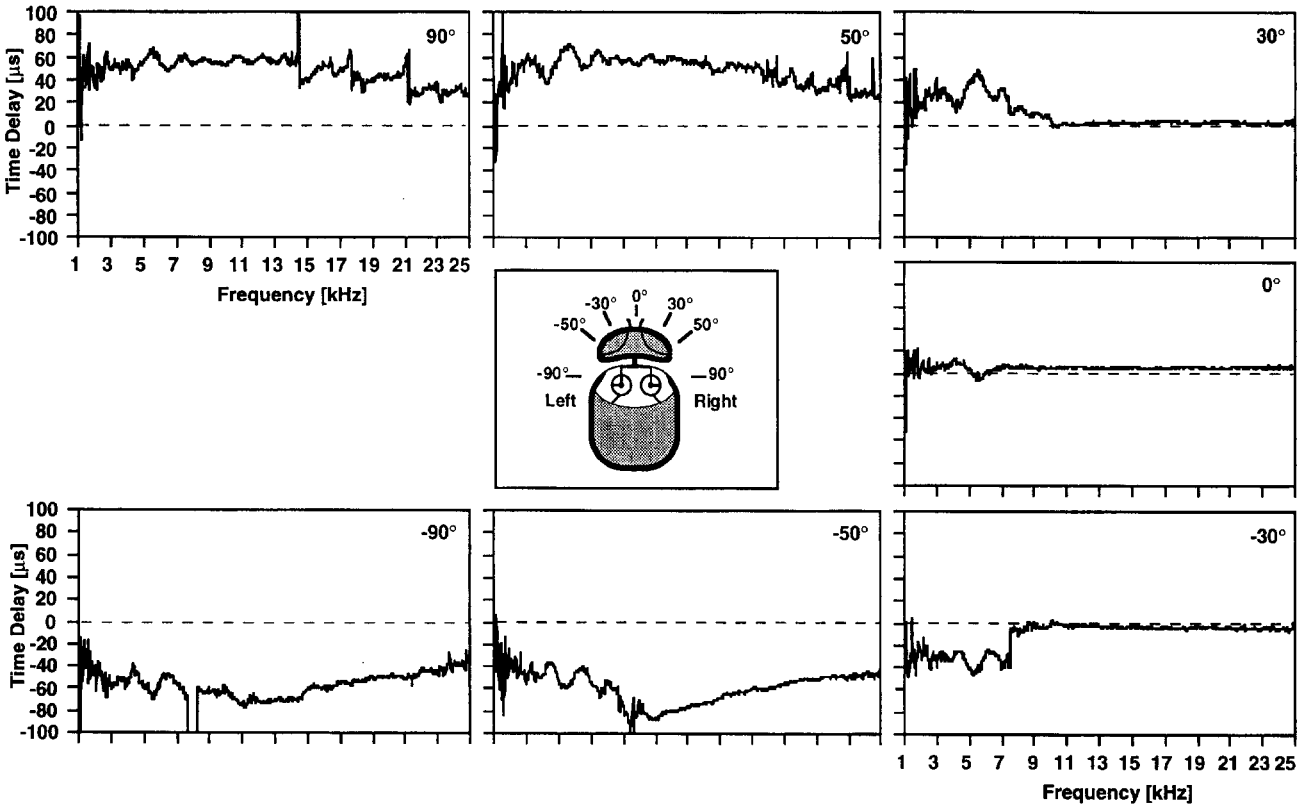

Fig. 10 Time delay between the tympanal pits as a function of frequency for different angles of sound incidence. Conventions as in Fig. 9. Positive time delays indicate a lead by the TP which is closer to the sound source. The frequency and time delay scales are the same for all panels

side experiences inward and outward motion, while the contralateral side vibrates relatively little (Fig. 13D).

Altogether, these results show interaural amplitude and time differences in the mechanical response on the order of 13 dB and 50 μs. In response to an incident sound arriving from one side, the peripheral auditory apparatus of the fly *O. ochracea* vibrates asymmetrically, thus providing, at the mechanical level, cues that are much larger than those available in the sound field.

Neural time delay

To investigate whether the observed interaural differences in the mechanical response of the fly's tympanal ears is reflected at the level of the nervous system, neurophysiological recordings were made from primary sensory neurons. Figure 14 shows the activity of auditory afferent neurons from the fly's left frontal nerve when sound is played from the left (ipsilateral) side or the right (contralateral) side. The time at which the incident sound reaches each ear is monitored with a probe microphone directly facing the tympanal membranes. The actual difference in the time of arrival of the incident acoustic waves at the tympana is 2 μs (Fig. 14, upper two curves). When the sound source is switched from left to right, the same auditory afferent (left side) fired with a difference in latency of 320 μs (lower two curves). For ipsi- and contralateral angles of incidence of 90°, the difference in the neural time delay is 313 ± 137 μs (sd, $n = 6$ animals). These results show that the mechanical delay of 50 μs and interaural amplitude differences measured at the tympanal pits are converted into a neural delay sufficiently large to provide directional neural information. Furthermore, this demonstrates the directional sensitivity of the fly's ears at the level of the primary auditory afferents. This has been confirmed in additional recordings from single afferent fibers (Oshinsky and Hoy 1995).

Discussion

Methodological considerations

It has long been known that diffraction around the head or the body plays an important role in the directional sensitivity of auditory systems (Rayleigh 1907). In most laboratory experiments involving insect preparations, micropositioning equipment (micromanipulators for electrodes, fixtures, microphones, microphone preamplifiers, etc.) are often large and close enough to the preparation to create significant pressure

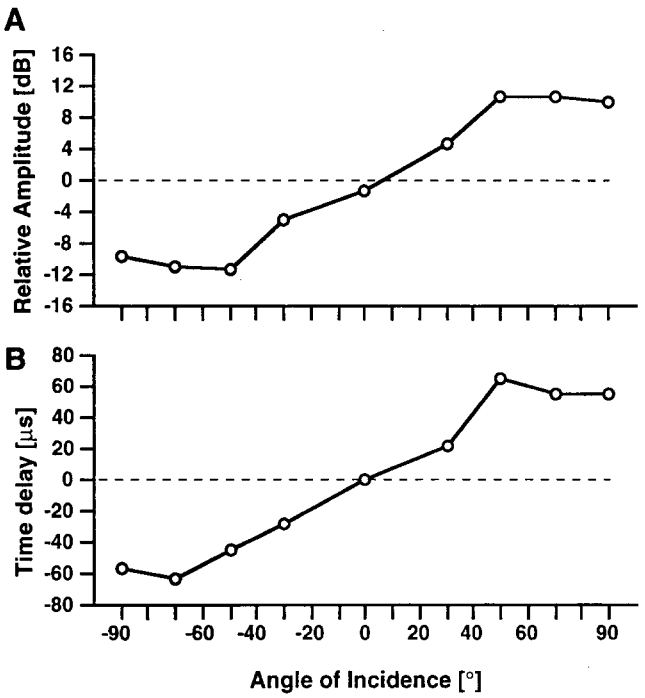

Fig. 11A, B Interaural amplitude and time differences for different angles of incidence at 5 kHz. **A** Difference in the response amplitude between the ipsi- and contralateral tympanal pits. **B** Time delay between the ipsi- and contralateral tympanal pits. Positive values indicate greater amplitudes, or an earlier response, for the animal's right hearing organ. Data are averages from 5 animals

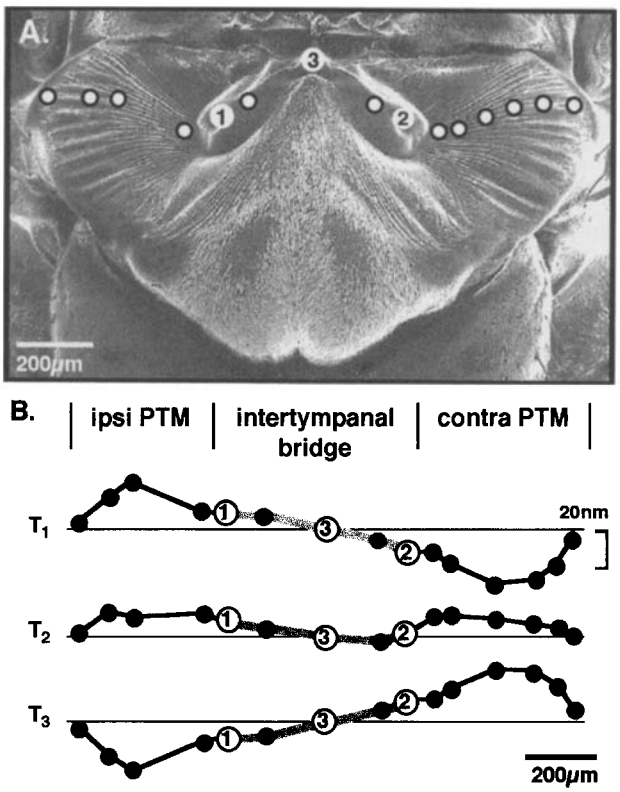

Fig. 12A, B Mechanical displacement of the tympanal ears. **A** Scanning electron micrograph showing the points of measurement across the two tympanal membranes and the intertympanal bridge. The dots numbered ① and ② indicate the ipsi- and contralateral tympanal pits, respectively. Dot ③ points to the center of the intertympanal bridge (the pivot). **B** Mechanical displacement in response to a 5 kHz incident sound. Data are from the transfer functions between the laser signal and the input pressure at 5 kHz. The segment between dots ① and ② represent the intertympanal bridge (see **A**). T_1, T_2 and T_3 refer to the times of minimal, zero-crossing and maximal ipsilateral pressure of the 5 kHz sound (200 µs period). *Vertical scale bar* (20 nm) indicates the linear mechanical displacement

alterations in the sound field. Measurements meant to quantify the homogeneity of the sound field and diffractive effects (i.e. Fig. 3, Robert 1989) clearly indicate the importance of careful acoustic calibrations. Reflections and diffractions inherent in any experimental situation can drastically affect the sound field in the vicinity of the insect and produce unexpected under- and over-pressures easily exceeding 10 dB. Thus, the actual sound pressure that an insect's auditory system experiences may not be that measured by a calibration microphone positioned even just a few centimeters away from the preparation.

In insects, such considerations are especially critical since the relevant frequencies often are above 10 kHz, above which any nearby object larger than 5 mm will introduce significant reflections and diffraction. However, there is no simple "rule of thumb" (which could replace actual measurements) that can be applied to assess or predict the extent of diffraction and reflection in a sound field or near the body of an insect. In most situations, it seems therefore that the a priori qualification (as often seen in the literature) of a sound field as "anechoic" or "free-field" may be incorrect. Careful calibration procedures, assessing the presence of standing waves, even for lower frequencies such as 5 kHz (Fig. 3), are necessary to reliably quantify the input pressure to the system under investigation (Michelsen et al. 1994). It is not only the directional properties of an auditory system that are affected by unquantified acoustic conditions. For instance, measurements of sensory thresholds at the neuronal and/or behavioral level are also subject to errors due to diffraction.

In the present study, it was necessary to establish that no diffractive or reflective effects could account for the interaural differences observed by laser vibrometry. Sound field measurements made at the location of the fly indicate the lack of diffractive effects at 5 kHz (Fig. 3A, B). However, even at this frequency, a slight standing wave builds up, indicating the presence of some echoing. Nevertheless, the variation in pressure over the entire plane measured is not greater than 1.5 dB (sd: 0.4) for 5 kHz, and 3.8 dB (sd: 0.7) for 20 kHz. Also, no significant pressure variations at 5 kHz could be measured with the probe microphones positioned exactly across the fly's body or at its ears. This is in accordance with the theory of diffraction whereby

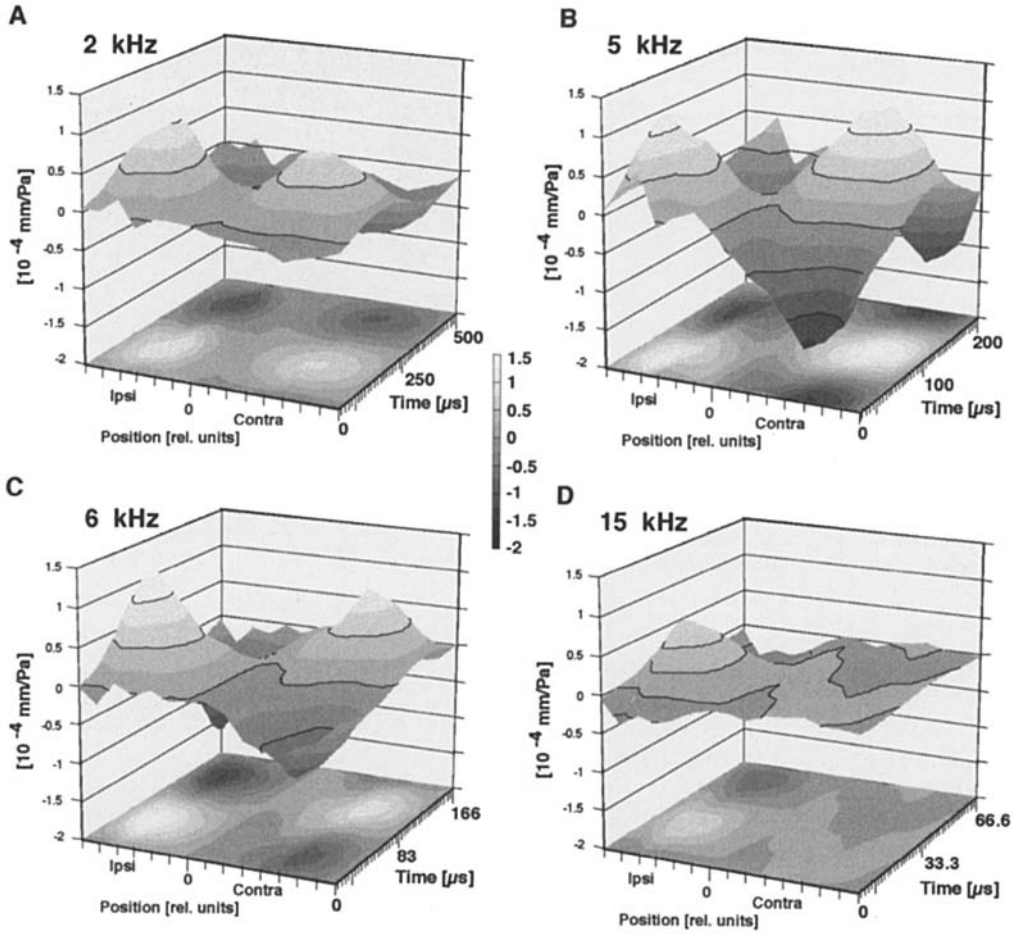

Fig. 13A–D Mechanical displacement of the tympanal ears at 2, 5, 6 and 15 kHz, shown as deflection shapes as a function of time. The data are shown as 3-D contour plots where the "position" axis indicates the ipsilateral and contralateral locations of the measured point (same as in Fig. 12A), the mechanical displacement is given in 10^{-4} mm/Pa along the vertical axis, and the time axis represents one period of the chosen frequency. Positive displacement values indicate outward displacement of the tympanal membranes. Note that the time scales are different for each frequency. The angle of incidence of the sound stimulus is 45°

a solid body 100 times smaller than the wavelength of the incident sound would have only negligible diffractive effects (Morse and Ingard 1968).

Interaural amplitude and time differences

The ears of ormiine flies are atypical tympanal organs because of their extreme close proximity to each other and because the auditory sensory organs are in an unpartitioned air sac (Lakes-Harlan and Heller 1992; Robert et al. 1992, 1994; Edgecomb et al. 1995). Most importantly, the two bilateral tympanal membranes are linked to each other across the midline through the presternum (Edgecomb et al. 1995), a sclerite functionally identified as the intertympanal bridge (Fig. 15A).

In response to an incident sound, the tympanal membranes of *O. ochracea* and their associated sclerite, the intertympanal bridge, experience mechanical displacements that demonstrate their role in the peripheral-most function of an hearing organ: the conversion of acoustic energy into mechanical energy. The ipsilateral tympanal membrane responds, at frequencies above 5 kHz, with an amplitude displacement on average 13 dB higher than the contralateral tympanal membrane. Similar bilateral differences were observed in the amplitude of the mechanical response of the tympanal pits. Given the small size of the fly and the direct structural connection of the tympanal pits to the auditory sensory organs, the asymmetry in the vibrational patterns confers directional sensitivity upon the hearing organs of this fly.

In addition to a level difference in the mechanical response of the intertympanal bridge system, the ipsilateral mechanical response leads the contralateral one by some 50 μs (Fig. 7B). This unexpectedly large time delay is nearly 50 times larger than the interaural difference in the time of arrival in the sound pressure measured at each tympanal pit (Fig. 7A). Independent

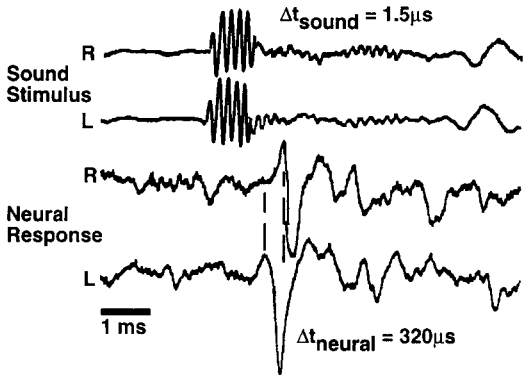

Fig. 14 Directionality measured at the level of the primary auditory afferents. *Top two traces*: sound pressure at the tympanal pits measured with the probe microphones for a stimulus from the right (*R*) or the left (*L*) speaker. The measured time delay between the two incident sound pressures is 1.5 μs. *Bottom two traces*: extracellular neurophysiological recording of primary afferents from the fly's left auditory nerve in response to sound from the right side (*R*) or the left side (*L*). The measured neural time delay is 320 μs

experiments using random noise stimuli also show a 50–60 μs bilateral mechanical delay for frequencies ranging from 3 to 25 kHz (Fig. 8). The observed sensitivity of the mechanical response to the angle of incidence of the sound pressure (Figs. 9, 10, 11) is consistent with the idea that these ears are directional receivers.

As previously argued, these interaural amplitude and time differences cannot be due to heterogeneities in the sound field surrounding the fly, and therefore must reflect the dynamic properties of the tympanal system itself.

Directional cues for neural coding

The mechanical response of the tympanal membranes and intertympanal bridge results in interaural time and

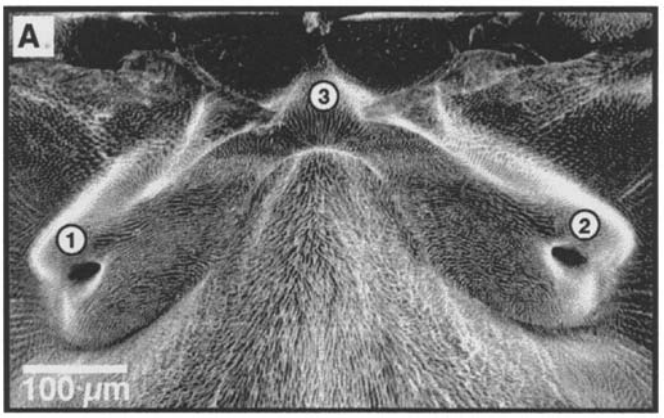

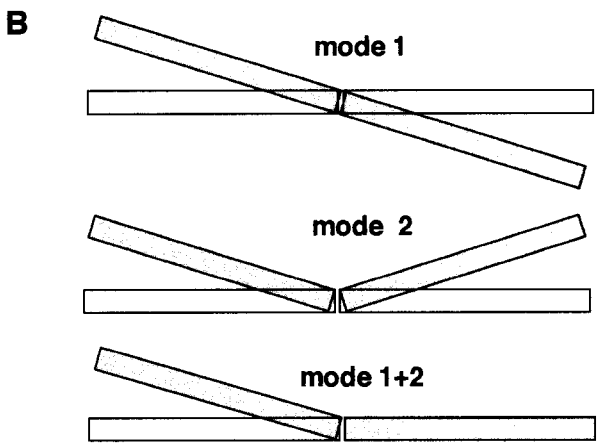

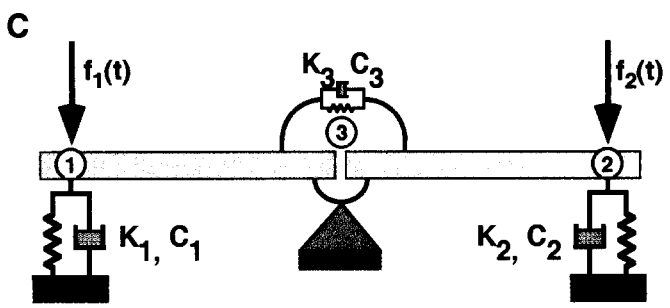

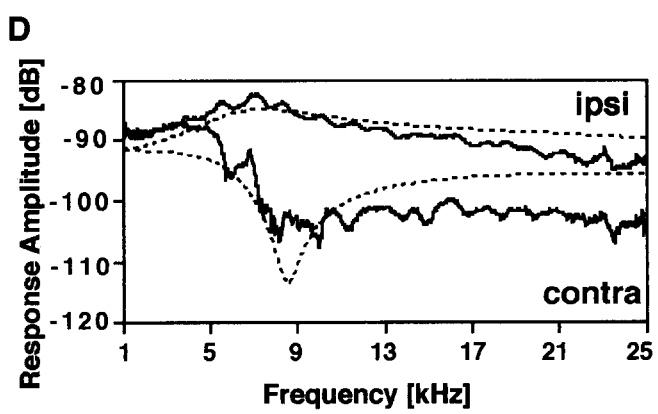

Fig. 15A–D Scanning electron micrograph of the intertympanal bridge, modes of vibration and mechanical analogue. **A** Close-up of the intertympanal bridge of *O. ochracea*. Dots ① and ② indicate the position of the tympanal pits. Dot ③ shows the pivot point (fulcrum) of the intertympanal bridge. **B** Modes of vibration of the intertympanal bridge. The first mode involves rocking of the bridge about the fulcrum. This mode is dominant at intermediate frequencies (5–7 kHz). The second mode is a translational bending motion in which the intertympanal bridge bends at the fulcrum and the two sides move in opposite directions; this mode dominates at lower frequencies (2 kHz). At higher frequencies (15 kHz), the combination of these two modes results in an hybrid motion where the ipsilateral side is set in motion and the contralateral side remains relatively immobile. **C** Mechanical analogue in which the intertympanal bridge is idealized by two beams connected by a torsional spring. Dots ① and ② at the end of each beam indicate the position of the tympanal pits. Dot ③ is the pivot point. Constants k_1, c_1, k_2, c_2, k_3, c_3 are spring and dash-pot constants (see Appendix). The *arrows* $f_1(t)$ and $f_2(t)$ represent the force of the acoustic pressure field applied to each tympanal systems. **D** Amplitude spectra of the predicted and measured mechanical response of the ipsi- and contralateral tympanal pits in response to sound stimulation at 45° azimuth. *Solid lines*: measured response. *Stippled lines*: predicted response. Response amplitude: − 90 dB is 31.6 nm/Pa. See Appendix for driving equations of the model and parameters

amplitude differences (respectively 50 μs and 3–13 dB) at the tympanal pits that are the cues for directional sensitivity. A priori, it may seem unlikely that a delay of 50 μs alone is sufficient to account for reliable directional coding between the ipsi- and contralateral mechanoreceptive organs. However, associated with this delay is an interaural amplitude difference in the mechanical response that is certainly sufficient to provide cues for directionality. Our physiological experiments show that the directional cues available at the peripheral level (e.g. the mechanical response of the tympanal pits) can be used by the mechanoreceptors of the sensory organs to encode directionality. In effect, the time delay between the primary afferents reaches about 300 μs (Fig. 14), a delay that is within the temporal resolution of an insect nervous system (Mörchen et al. 1978). The cues that are effective at the mechanoreceptor cells may however be different from those measured at the tympanal pits. Two phenomena could contribute to the larger relative delay between the primary afferents. First, a further mechanical delay may take place in the cuticular auditory apodeme which connects the tympanal pit to the scolopidial sensory organ. Second, an amplitude-dependent delay of activation of the sensory neurons may account for the increased delay measured at the primary afferents. Biomechanical and physiological experiments are in progress that investigate the mechanical response of the sensory organs and the neural coding of time and intensity at the primary afferents (Oshinsky and Hoy 1995).

The intertympanal mechanical coupling

The analysis of the relative displacements measured at multiple points across the ears illustrates the dynamics of tympanal and intertympanal bridge motion (Figs. 12, 13). As shown in Fig. 12B, the intertympanal bridge undergoes an asymmetrical displacement about its center (dot #3), much like a flexible see-saw rocking back and forth about its fulcrum. How this asymmetrical mechanical response comes about is described in detail using a mathematical model in Miles et al. (1995). In the following we will attempt a qualitative description of the system.

A key feature of the mechanical system is the flexibility of the intertympanal bridge. This flexibility can be seen by noting that if the intertympanal bridge were rigid, its oscillations at 5 kHz would produce a phase delay between its extremities (the tympanal pits) of half a period (180° phase shift, i.e. 100 μs). Furthermore, the extremities of a rigid see-saw would oscillate about the fulcrum with equal amplitudes which, in fact, is not observed over a wide frequency range (Fig. 6). Also, at 5 kHz the time delay measured between the tympanal pits is 50 μs (Fig. 7B) rather than 100 μs. This shows that the phase delay between the tympanal pits is 90° rather than 180° as would be the case for a rigid lever.

The flexibility of the intertympanal bridge is also apparent in the different patterns of vibration observed for different frequencies (Fig. 13A–D). At low frequency (around 2 kHz for this system), the two arms of the see-saw move in unison, with equal amplitudes, while the intertympanal bridge bends in the middle (Fig. 13A). At intermediate frequencies (5–6 kHz), the deflection shapes indicate a rocking motion (Fig. 13B, C) While the ipsilateral tympanal pit is deflected outward, the contralateral pit experiences an inward deflection. At higher frequency (15 kHz), the side ipsilateral to the sound is deflected inwards and outwards while the contralateral side remains relatively immobile (Fig. 13D). Altogether, these observations demonstrate that the intertympanal bridge acts like a flexible lever.

To see how this flexible coupling between the tympana results in asymmetrical response, note that the general motion of this system can be decomposed into two natural modes of vibration (see Miles et al. 1995, Fig. 15B and Appendix). One mode consists of a pure rocking motion of the bridge about its fulcrum (Fig. 15B, mode 1). In our model of the system (Miles et al. 1995) this mode is predicted to have a resonant frequency of 7.1 kHz. The second mode consists of both ends of the bridge translating in-phase and is predicted to have a resonant frequency of 31 kHz (Fig. 15B, mode 2). The response of the system at any frequency may be represented by a linear combination of these two natural motions. The relative contribution of each mode to the total system response depends on how close the frequency of the incident sound is to the resonant frequency of the mode and how well the excitation field (the driving sound pressure) couples to the motion of the mode. When the excitation frequency is close to the resonant frequency the response will tend to be greater than at any other frequencies (unless the system is heavily damped which is not the case here). In the two modes of this system, the coupling of the excitation field to each mode plays an important role in determining the amplitude of the mode's motion.

The ability of the incident sound pressures to drive each of the modes depends on the relative phase of the pressures acting on the tympana. These incident sound pressures, $p_1(t)$ and $p_2(t)$ can be regarded as two sinusoidally varying point forces, $f_1(t)$ acting on the ipsilateral end of the intertympanal bridge and $f_2(t)$ acting on the contralateral end (Fig. 15A, C). Due to the small interaural distance, these forces are slightly delayed in time (ca. 2 μs). Thus, $f_1(t)$ will act on the ipsilateral pit shortly before $f_2(t)$ will act on the contralateral pit. In the same manner that a see-saw is put out of static equilibrium by two weights of equal mass deposited at different times on each of its ends, these forces will provoke a rocking motion of the bridge. As one arm of the bridge is deflected downward, the other arm will move upward due to the stiffness of the bridge (Fig. 15B, mode 1). In the steady state, the rocking mode is sensitive only to the difference in the forces

applied on either side. The translating mode responds only to the sum of the two forces. Forces that have equal amplitude but are applied in opposite directions will not excite the translating mode. The relative contributions of these modes depend in a somewhat complicated way on the difference or sum of excitation forces and on the resonant properties of the system (see Miles et al. 1995).

It is essential to note here that, for a given interaural distance, the instantaneous amplitude difference between $f_1(t)$ and $f_2(t)$ will depend on the frequency of the incident sound. At low frequencies (2 kHz), the difference in these forces will be smaller than at higher frequencies (5–6, 15 kHz). At 2 kHz, the phase delay is 1° for an intertympanal distance of 0.5 mm. As a result $f_1(t)$ and $f_2(t)$ will act together with nearly the same amplitude and in relative synchrony on both sides of the bridge, thus forcing it to respond predominantly in the translating mode. At 5 kHz, the phase delay is larger (2.6°), resulting in a larger difference between $f_1(t)$ and $f_2(t)$ and therefore will more effectively drive the rocking mode. In addition, the driving frequency is closer to the natural frequency of the rocking mode (estimated to be close to 7 kHz in the model). As a result, it becomes easier for the difference in the forces, $f_1(t) - f_2(t)$ to elicit the rocking motion of the bridge and thus the rocking mode will dominate the overall pattern of vibration. At higher frequencies (15 kHz), the difference in the instantaneous forces applied to the bridge is even larger (7.6° phase shift), which further enhances the ability of the sound to excite the rocking mode. However, at these frequencies, the rocking mode is being driven above its resonant frequency which will cause a decrease in response level with increasing frequency. The net effect is for the rocking mode to continue to contribute to the response. In addition, this frequency range is sufficiently close to the resonant frequency of the translating mode (31 kHz) that this mode is driven with roughly the same amplitude as the rocking mode. The additive and equal contribution of both modes results in the deflection shapes observed for higher frequencies (i.e. 15 kHz). If the amplitudes and phases of the two modes are approximately equal then the modes will tend to add together for one tympanal ear and cancel for the other (Fig. 13D, Fig. 15B, mode 1 + 2).

The anatomy (Figs. 6A, 15A) and the mechanical response (Fig. 13) of the tympanal membranes and the intertympanal bridge led to the development of a simple mechanical analogue described in Fig. 15C. This model helps to visualize the vibratory behavior of the tympanal system in a sound field. The mathematical treatment of this model is also presented briefly in the Appendix. A more complete analysis and the derivation of the equations is reported in Miles et al. (1995). In this model, the flexible intertympanal bridge is represented by two rigid bars connected medially by a torsional spring and a dash pot (Fig. 15A, C). Both extremities of the bridge are connected to a spring and a dash-pot that represent the stiffness and damping characteristics of the auditory apodeme and sensory organs attached to the tympanal pits. As seen in Fig. 15D, this analytical model can predict reasonably well the measured data and is consistent with the idea that intertympanal mechanical coupling is sufficient to account for directional hearing in *O. ochracea*.

The empirical evidence provided in this paper clearly illustrates the unusual rocking and translational motions of the coupled tympanal membranes. The deflection shapes and the mechanical analogue strongly suggest that the flexible intertympanal bridge provides the basis for the measured interaural differences. However, the possibility exists that the air space behind both tympanal membranes may have a sufficient stiffness to play a role in the directional response (as would be the case for the acoustically coupled ears of pressure-difference receivers). This possibility is being investigated and will be presented fully in a subsequent paper (Robert et al., unpublished). In short, these experiments show that opening the air sac backing the tympanal membranes (thus greatly reducing the stiffness of the putative air spring behind the tympanal membranes) does not affect the mechanical response properties of this system. These experiments demonstrate that the air column behind the membranes is not involved in the asymmetrical response of the tympana. It is thus unlikely that a pressure-difference receiver system, in the conventional sense (Fletcher 1992), operates in *O. ochracea*.

In conclusion, the present results provide strong evidence that the mechanical response of the peripheral auditory apparatus of the fly *O. ochracea* relies on the coupling of the two tympanal membranes by the intertympanal bridge, resulting in a unique mechanism for directional hearing.

Acknowledgements Many thanks are due to P.A. Faure and T.G. Forrest for their critical and constructive comments on the manuscript. The authors are also grateful to T. Tieu and Y. Xu for assistance in data acquisition and processing, M. Read for scanning electron microscopy, and G.-A. Haldimann for the light-scanning micrographs. The authors were supported as follows: DR and RRH by grants from NINDCD DC00103 and Hatch NYC-191403, RNM and RRH by NSF grant BCS9315854 and DR by the Swiss National Fonds and the Janggen-Pöhn Foundation.

Appendix

The analytical model

As pointed out in the discussion, the vibratory behavior of the intertympanal bridge can be decomposed into its two natural modes of vibration. In the first mode both tympanal pits are rocking about the pivot point so that they move exactly out of phase with different amplitudes (Fig. 15B, mode 1). In the second mode, the

tympanal pits are moving in phase and with equal amplitudes (Fig. 15B, mode 2). It can be shown that the observed interaural differences in the mechanical response are a result of the addition of these two natural modes of vibration for the ipsilateral side and their subtraction for the contralateral side (Miles et al. 1995).

A harmonic plane acoustic wave will produce a pressure at the location of the pivot point which may be expressed as $p(t) = Psin(\omega t)$, where P is the amplitude of the acoustic pressure and ω is the frequency in radian/s. The pressure applied at the ipsilateral pit will be $p_1(t) = Psin(\omega t + \omega\tau/2)$ and that at the contralateral tympanal pit will be $p_2(t) = Psin(\omega t - \omega\tau/2)$ where τ is the interaural time delay in the acoustic pressure. The natural mode which consists of pure rocking motion (mode 1) will be driven only by the difference in these pressures, $p_1(t) - p_2(t) = P\ (sin(\omega t + \tau/2) - sin(\omega\tau - \tau/2)) = 2Pcos(\omega t)sin(\omega\tau/2)$. In contrast, the translational mode (mode 2) is driven by the sum of the two pressures $p_1(t) + p_2(t) = 2Psin(\omega t)cos(\omega\tau/2)$. The force applied to the rocking mode (out-of-phase) is proportional to $cos(\omega t)$, and that applied to the translational mode is proportional to $sin(\omega t)$. Therefore, the two modes are driven by effective forces which differ in phase by 90°. The responses in the steady-state (after initial transients) of the ipsi- and contralateral tympanal pits may be expressed as a linear combination of the responses to these forces:

$$x_1(t) = A_t\sin(\omega t + \phi_t) + A_r\cos(\omega t + \phi_r)$$
$$x_2(t) = A_t\sin(\omega t + \phi_t) - A_r\cos(\omega t + \phi_r) \quad [1]$$

where A_r is the amplitude of the response of the rocking mode and A_t is the amplitude of the response of the translating mode. These amplitudes may be expressed in terms of the excitation frequency and the system parameters as

$$A_r = 2Ps/m\left(\frac{\sin(\omega\tau/2)}{\sqrt{(\omega_r^2 - \omega^2)^2 + (2\omega_r\xi_r\omega)^2}}\right)$$
$$A_t = 2Ps/m\left(\frac{\cos(\omega\tau/2)}{\sqrt{(\omega_t^2 - \omega^2)^2 + (2\omega_t\xi_t\omega)^2}}\right) \quad [2]$$

where ω_r and ω_t are the natural frequencies of the rocking mode and the translation mode respectively, ξ_r and ξ_t are the modal damping ratios (ratio of the equivalent modal viscous dash-pot constant to the critical dash-pot constant) of the rocking and translation modes respectively. See "Numerical simulation" section for the determination of ω and ξ. s is the surface area of the tympanal membrane and m is the effective mass. The phase constants in Eq. [1] are

$$\phi_r = -\arctan\left(\frac{2\omega_r\xi_r\omega}{\omega_r^2 - \omega^2}\right)$$
$$\phi_t = -\arctan\left(\frac{2\omega_t\xi_t\omega}{\omega_t^2 - \omega^2}\right). \quad [3]$$

It can be seen in Eq. [1] that the expressions for the motion of the tympanal pits differ only in that the term associated with the rocking motion (with resonant frequency ω_r) adds for the ipsilateral tympanum (x_1) while it subtracts for the contralateral tympanum (x_2). While the consequences of this will depend on some other parameters of the system (such as ω_t, ξ_t, ω_r, ξ_r) it is clear that the two transfer functions can differ substantially even though the time delay in the incident sound τ is quite small. This can lead to significant interaural differences in the mechanical response of the tympanal pits. The complete derivation of this analytical model has been published elsewhere (Miles et al. 1995).

Numerical simulation

The physical dimensions used for the numerical simulation, (e.g. length, width and thickness of the intertympanal bridge, sensory organs and associated structures) were measured from scanning electron micrographs and freshly dissected animals. Calculations of the volume of these structures and estimation of their specific density (close to water) allowed for an estimation of the effective lumped mass m at each tympanal pit of 2.88×10^{-10} kg. The surface area of the tympanal membranes is 0.288×10^{-6} m^2 (Robert et al. 1994). Several physical parameters could not be measured by independent methods and have been given approximate values: $k_1 = k_2 = 0.576$ N/m, $k_3 = 5.18$ N/m, $c_1 = c_2 = c = 1.15 \times 10^{-5}$ Ns/m, $c_3 = 2.88 \times 10^{-5}$ Ns/m. From these constants k_1, k_2, k_3, c_1, c_2 and c_3 the natural frequencies can be calculated by $\omega_r = \sqrt{k/m}$; $\omega_t = \sqrt{(k + 2k_3)/m}$; $\xi_r = c/(\omega_r m)$ and $\xi_t = (c + 2c_3)/(\omega_t m)$; $\omega_r = 7.114$ kHz, $\omega_t = 31.035$ kHz, and the two modal loss factors take the value $\xi_r = 0.89$ and $\xi_t = 1.23$. Interestingly, the estimated system parameters approach damping ratios close to one, indicating that this system is nearly critically damped. Critical damping is indeed very reasonable for mechanical systems (such as hearing organs) with high temporal resolution. The time delay in the pressures applied to the tympana was taken to be $\tau = 2.5$ μs.

Using these parameters, the mathematical model given in Eq. [2] provides the simulated response shown in Fig. 15D. For lower frequencies, the model predicts fairly well the mechanical response of the tympanal pits. At higher frequencies (> 13 kHz) predictions are

less accurate (the measured response of the contralateral pit is different from the simulated response). However, the model still accounts for the observed interaural amplitude differences.

References

Bennet-Clark HC (1984) Insect hearing: Acoustics and transduction. In: Lewis T (ed) Insect communication. Academic Press, London

Cade WH (1975) Acoustically orienting parasitoid: fly phonotaxis to cricket song. Science 190: 1312–1313

Calford MB, Piddington RW (1988) Avian interaural canal enhances interaural delay. J Comp Physiol A 162: 503–510

Coles RB, Guppy A (1988) Directional hearing in the barn owl (*Tyto alba*). J Comp Physiol A 163: 117–133

Coles RB, Gower DM, Boyd PJ, Lewis DB (1982) Acoustic transmission through the head of the common mole, *Talpa europaea*. J Exp Biol 101: 337–341

Edgecomb RS, Robert D, Read M, Hoy RR (1995) The tympanal hearing organ of a fly: phylogenetic analysis of its morphological origins. Cell Tissue Res 282: 251–268

Eggermont JJ (1988) Mechanisms of sound localization in anurans. In: Fritzsch B, Ryan MJ, Wilczynski W, Hetherington TE, Walkowiak W (eds) The evolution of the amphibian auditory system. John Wiley, New York Chichester Brisbane Toronto Singapore, pp 307–336

Fletcher NH (1992) Acoustic systems in biology. Oxford University Press

Fonseca P (1993) Directional hearing of a cicada: biophyical aspects. J Comp Physiol A 172: 767–774

Henson OW (1974) Comparative anatomy of the middle ear. In: Keidel WD, Neff WD (eds) Handbook of sensory physiology, vol V/1. Springer, Berlin Heidelberg New York, pp 39–110

Hill KG, Boyan GS (1977) Sensitivity to frequency and direction of sound in the auditory system of crickets. J Comp Physiol 121: 79–97

Hill KG, Lewis DB, Hutchings ME, Coles RB (1980) Directional hearing in the Japanese quail (*Coturnix coturnix japonica*) I. Acoustic properties of the auditory system. J Exp Biol 86: 135–151

Hoy RR, Robert D (1996) Tympanal hearing in insects. Ann Rev Entomol 41: 433–450

Knudsen EI (1980) Sound localization in birds. In: Popper AN, Fay RR (eds) Comparative studies of hearing in vertebrates. Springer, Berlin Heidelberg New York, pp 289–322

Lakes-Harlan R, Heller K-G (1992) Ultrasound sensitive ears in a parasitoid fly. Naturwissenschaften 79: 224–226

Löhe G, Kleindienst HU (1994) The role of the medial septum in the acoustic trachea of the cricket *Gryllus bimaculatus*. II. Influence on directionality of the auditory system. J. Comp Physiol A 174: 601–606

Michel K (1974) Das Tympanalorgan von *Gryllus bimaculatus* Degeer (Saltatoria: Gryllidae). Z Morph Tiere 77: 285–315

Michel K (1975) Das tympanalorgan von *Cicada omi* (Cicadina, Homoptera). Zoomorphologie 82: 63–78

Michelsen A (1994) Directional hearing in crickets and other small animals. In: Schildberger K, Elsner N (eds) Fortschritte der Zoologie, vol 39: Neural basis of behavioural adaptations. Fischer, Stuttgart, pp 195–207

Michelsen A, Larsen ON (1985) Hearing and sound. In: Kerkut G, Gilbert L (eds) Comprehensive insect physiology, biochemistry, and pharmacology, vol 6. Pergamon, New York, pp 495–556

Michelsen A, Popov AV, Lewis B (1994) Physics of directional hearing in the cricket *Gryllus bimaculatus*. J Comp Physiol A 175: 153–164

Middlebrooks JC, Green DM (1991) Sound localization by human listeners. Annu Rev Psychol 42: 135–159

Middlebrooks JC, Makous JC, Green DM (1989) Directional sensitivity of sound pressure levels in the human ear canal. J Acoust Soc Am 86: 89–108

Miles RN, Robert D, Hoy RR (1995) Mechanically coupled ears for directional hearing in the parasitoid fly *O. ochracea*. J Acoust Soc Am 98(6): 3059–3070

Moiseff A, Konishi M (1981) Neuronal and behavioral sensitivity to binaural time differences in the owl. J Neurosci 1: 40–48

Mörchen A, Rheinländer J, Schwartzkopff J (1978) Latency shift in insect auditory fibers. Naturwissenschaften 65: 657

Morse PM, Ingard KU (1968) Theoretical acoustics. McGraw Hill, New York, pp 418–422

Narins PM, Ehret G, Tautz J (1988) Accessory pathway for sound transfer in a neotropical frog. Proc Natl Acad Sci USA 85: 1508–1512

Oshinsky ML, Hoy RR (1995) Response properties of auditory afferents in the fly *O. ochracea*. In: Burrows M, Matheson T, Newland PL, Schuppe H (eds) Nervous systems and behaviour. Thieme, Stuttgart New York, p 359

Rayleigh Lord (1907) On our perception of sound direction. Philos Mag 13: 214–232

Robert D (1989) The auditory behaviour of flying locusts. J Exp Biol 147: 279–301

Robert D, Amoroso J, Hoy RR (1992) The evolutionary convergence of hearing in a parasitoid fly and its cricket host. Science 258: 1135–1137

Robert D, Read MP, Hoy RR (1994a) The tympanal hearing organ of the parasitoid fly *Ormia ochracea* (Diptera, Tachinidae, Ormiini). Cell Tissue Res 275: 63–78

Robert D, Miles RN, Hoy RR (1994b) A novel mechanism for directional hearing in a parasitoid fly. J Acoust Soc Am 96: 3296

Schlegel PA (1994) Azimuth estimates by human subjects under free-field and headphone conditions. Audiology 33: 93–116

Walker TJ (1986) Monitoring the flights of the field crickets (*Gryllus* spp.) and a tachinid fly (*Euphasiopterix ochracea*) in north Florida. Florida Entomol 69: 678–685

Walker TJ, Wineriter SA (1991) Hosts of a phonotactic parasitoid and levels of parasitism (Diptera: Tachinidae: *Ormia ochracea*). Fla Entomol 74: 554–559

Wendler G, Löhe G (1993) The role of the median septum in the acoustic trachea of the cricket *Gryllus bimaculatus*. I. Importance for efficient phonotaxis. J Comp Physiol A 173: 557–564

Wineriter SA, Walker TJ (1990) Rearing parasitoid flies (Diptera: Tachinidae Ormiini, *Ormia* spp.) Entomophaga 35: 621–632

Young D, Hill KG (1977) Structure and function of the auditory system of the cicada, *Cystosoma saundersii*. J Comp Physiol 117: 23–45